THE ASTROPHYSICAL JOURNAL, 345:871–880, 1989 October 15

CENTRAL STAR TEMPERATURES OF OPTICALLY THICK PLANETARY NEBULAE AND A DISTANCE-INDEPENDENT TEST OF DREDGE-UP THEORY

JAMES B. KALER
Department of Astronomy, University of Illinois

AND

GEORGE H. JACOBY
Kitt Peak National Observatory, National Optical Astronomy Observatories
Received 1988 October 31; accepted 1989 April 20

ABSTRACT

We calculate the effective temperatures and predict the V magnitudes of the central stars of 62 optically thick planetary nebulae by forcing agreement between the hydrogen and ionized helium Zanstra temperatures. Comparison to the measured V for 34 of the stars shows good agreement and validates the method for the other 28, for which no Zanstra analysis is available. In many cases the predicted V magnitudes are actually likely to be better than the currently measured values. The comparison suggests that optical depth and not an ultraviolet excess is the dominant cause of the Zanstra discrepancy. Nebular N/O correlates positively with effective temperature, demonstrating that the N/O–core mass relation rises more steeply than predicted by dredge-up theory.

Subject headings: nebulae: planetary — stars: abundances — stars: interiors — stars: luminosities

I. CENTRAL STAR TEMPERATURES

Among the most important parameters to know for stars are their temperatures. With the distances and magnitudes, and hence the luminosities, we can then place them on some form of H-R diagram for various tests of theories of stellar structure and evolution. The nuclei of planetary nebulae, as predecessors of white dwarfs, are critical to our understanding of stellar death. But these stars are so hot—all over 25,000 K, with some ranging to over 200,000 K—that standard forms of temperature analysis often fail: spectral gradients are all about the same in the optical and may not properly reflect temperature in the accessible ultraviolet, and emission features from hot winds may confuse the study of the stellar spectrum lines. The surrounding nebula, however, comes to the rescue. Since it is ionized by far-ultraviolet photons, whose number and energy distribution are exquisitely sensitive to temperature and luminosity, it can be used in a variety of ways to infer what the temperature ought to be.

The most commonly used method was developed by Zanstra (1927). In its modern usage (see Harman and Seaton 1966) the nebular Hβ flux yields the stellar UV flux beyond the hydrogen Lyman limit, and comparison with the stellar V magnitude gives the temperature. The method can be applied as well to ionized helium. If the nebula is optically thick, absorbing all ionizing radiation, and if the functional form of the energy distribution of the star is known, then the two Zanstra temperatures, T_Z(H) and T_Z(He II), must be equal. They rarely are: T_Z(He II) is almost always the higher. There are two possible explanations for this "Zanstra discrepancy": either the nebula is optically thick in the He^+ Lyman continuum but thin in that of hydrogen (Harman and Seaton 1966; Kaler 1983*b*), or there is an excess of radiation shortward of 228 Å relative to the true effective temperature (Henry and Shipman 1986; Méndez *et al.* 1988). We will argue below (§ II) for the first of these two cases.

First, however, note that the Zanstra method requires measurement of a very elusive stellar property, the magnitude. For most stars, it is a trivial thing to determine, but for planetary nuclei, the bright nebula gets in the way, and under some circumstances can hide the star altogether. Errors in the literature of one or two magnitudes are not uncommon. For many planetaries for which the star is barely detectable, or unseen, it is necessary to use a method that avoids it completely. Three such are available. The most popular, developed by Stoy (1933), uses the energy balance to infer temperature (i.e., the heating rate must equal the observed cooling rate): see Kaler (1976*a*) and Preite-Martinez and Pottasch (1983). The distribution of nebular ionic abundances, which must reflect the distribution of input energy, has also been used (Natta, Pottasch, and Preite-Martinez 1983). Both of these methods have the disadvantage that a considerable amount of nebular data is needed. In addition, the Stoy procedure suffers from theoretical difficulties that involve the interlocking of hydrogen and helium ionization.

Before proceeding in § II to the third way of avoiding the star—the subject of this paper—we direct the reader to two other broadly discussed *direct* methods of temperature measurement. First, this parameter can be evaluated by fitting theoretical absorption line profiles to the observed, as has been elegantly done by Méndez *et al.* (1988). These temperatures tend to be below T_Z(He II), rather between T_Z(H) and T_Z(He II) (see Kaler 1989), and support the notion of the UV excess. The method is rather severely limited to bright absorption-line stars, however. Second, the observed UV continuum can be fitted by a selected energy distribution (e.g., Harrington *et al.* 1982; Clegg and Seaton 1983). However, the correct model seems to elude us: blackbodies often give temperatures that are too high (Kaler and Feibelman 1985). The subject is further reviewed by Kaler (1985*a*, 1988).

II. CROSSOVER (AMBARTSUMYAN) TEMPERATURES

a) Concept

Now, for the third time, we avoid the star. Assume an optically thick hypothetical nebula. In the simple picture in which the central star behaves as a blackbody, with a sufficiently high

temperature, over about 60,000 K, $T_Z(\mathrm{H}) = T_Z(\mathrm{He\ II})$. If we then lower the optical depth, the nebula first thins in H-Lyman radiation ($\lambda < 912$ Å). The zone that contains He^{+2} lies interior to the He^+ shell, and simply expands, leaving the nebula thick in the He^+ Lyman continuum ($\lambda < 228$ Å). The result is that $T_Z(\mathrm{H})$ drops (since not all the photons are being captured), and $T_Z(\mathrm{He\ II})$ stays the same, or $T_Z(\mathrm{He\ II})/T_Z(\mathrm{H}) = R_Z$ increases from unity. Finally, the He^{+2} zone meets the edge of the nebula, He^+ Lyman photons escape, and $T_Z(\mathrm{He\ II})$ starts to drop, even as R_Z continues to rise (see Harman and Seaton 1966 and Kaler 1983*b*).

Next, allow the central star magnitude to change, holding other parameters constant, and begin with a value low enough so that $T_Z(\mathrm{H}) < T_Z(\mathrm{He\ II})$. As the magnitude is increased, (i.e. made fainter), the two Zanstra temperatures calculated from it must rise. (As the contrast between the nebular and stellar brightness increases, relatively more of the calculated stellar energy must be exiting in the ionizing far-UV.) The hydrogen temperature will increase the more rapidly of the two, and we can nearly always find a magnitude at which $T_Z(\mathrm{H}) = T_Z(\mathrm{He\ II})$. The graphs of $T_Z(\mathrm{H})$ and $T_Z(\mathrm{He\ II})$ versus V cross one another, hence the name we assign to it, the "crossover temperature." If the nebula is optically thin (which most planetaries containing doubly ionized helium appear to be) then $V(\mathrm{cross})$ must be too high, or rather will be an upper limit. If the nebula is indeed thick, however, we can measure T and predict V at the same time.

This method in effect uses the amount of He^{+2} relative to H^+ to imply temperature and is the simplest version of that used by Natta, Pottasch, and Preite-Martinez (1980). In practice, the He II λ4686/Hβ nebular flux ratio simply responds to temperature. The procedure was first suggested by Ambartsumyan (1932), and the results should properly be referred to as "Ambartsumyan temperatures," T_A, in parallel with "Zanstra" and "Stoy" temperatures. Once T_A is found from the original method, we may then apply the Zanstra procedure to find what V would be necessary to render $T_Z(\mathrm{H}) = T_Z(\mathrm{He\ II}) = T_A$. Nevertheless, we will hereafter refer to these temperatures and magnitudes as $T(\mathrm{cross})$ and $V(\mathrm{cross})$ since the terms are so descriptive of the method actually used.

The Ambartsumyan method has a significant recent literature. Ferland (1978) used it to derive temperatures for Nova Cygni (1975), and Iijima (1981) employed it in analysis of symbiotic stars. With the crossover method employed in this paper, Shaw and Kaler (1982) derived both the temperature and magnitude of the nucleus of NGC 7027, and Preite-Martinez and Pottasch (1983), in an interesting variation, predicted a magnitude for the central star of NGC 2440 by forcing equality between the Zanstra and Stoy temperatures. Reay *et al.* (1984) then used the crossover technique to find the magnitude and temperature for the nucleus of NGC 6565.

In a detailed paper on Zanstra temperatures, Stasińska and Tylenda (1986) critique the method and describe a possible pitfall. In the standard Zanstra method as developed by Harman and Seaton (1966), it is assumed that He^+ absorbs all the stellar radiation shortward of 228 Å and that each He^{++} recombination ultimately produces one H ionization, so that to derive each temperature we need only integrate from the ionization limit to infinity. However, Stasińska and Tylenda demonstrate that above 100,000 K, for the nebular models they use, He^+ is not the sole absorber of the He^+ Lyman continuum, and that more than one hydrogen-ionizing photon is created for every He^{++} recombination. The result is that the H and He II Zanstra temperatures are respectively too high and too low (the opposite of the Zanstra discrepancy), and that the Ambartsumyan temperature (from the He II/H I ratio) is lower yet. The differences become more pronounced with increasing temperature, such that $T(\mathrm{cross})$ would be over 25% too low at 200,000 K and 54% low at 250,000 K. This matter will be discussed further in the results below.

Finally, Golovatyi (1987) applied the Ambartsumyan method broadly to a number of planetaries, using both the He I/Hβ and He II/Hβ intensity ratios. We, however, restrict our study to He II, and, as our innovation, employ spectroscopic optical depth standards to ensure high optical thickness, which we describe next.

b) Optical Depth

We must first identify criteria for optically thick nebulae, and at the same time have some assurance that the Zanstra discrepancy is in fact caused by optical depth variation with wavelength and not by a UV excess. Both are provided in a study by Kaler (1983*b*) of large planetary nebulae that cover a wide range of optical thickness. All nebulae show effects of stratification, wherein the higher ionization states are concentrated toward the center, close to the nucleus. If a nebula is mass-bounded (optically thin), there may be no low-ionization species at all. At the extreme, some planetaries are filled with doubly ionized helium. If an object is ionization-bounded, however, the low-ionization species must appear as the last of the lower energy ionizing radiation is absorbed (see, for example, discussion by Osterbrock 1974 and Aller 1984). An optically thick object then must have a prominent outlying shell filled with O^+ and N^+. In addition, a thick object should have $T_Z(\mathrm{H}) = T_Z(\mathrm{He\ II})$.

Kaler (1983*b*) plotted the Zanstra temperature ratio, R_Z (which he called "TR"), against the dereddened strengths of [O II] λ3727 and [N II] λ6584 [in the form of 100 $F(\lambda3727)/F(\mathrm{H}\beta)$ and $F(\lambda6583)/F(\mathrm{H}\alpha)$]. In both cases, the λ3727 and λ6583 strengths correlate with R_Z exactly as qualitatively expected: R_Z is high when the lines are weak and approaches unity as they strengthen. If the Zanstra discrepancy were *generally* caused by a really significant UV excess, R_Z would approach a limit *greater* than 1 as these lines develop. But it does not: the limit is indeed very close to unity, with a small scatter below it as expected, a result of observational error. Of course the true limit could be greater than 1, and just appears to be lower because of observational scatter, but from Kaler's (1983*b*) error bars it cannot be too large: the limit seems almost certainly to be less than 1.2. Moreover, the Stasińska-Tylenda effect (§ II*a*) might lower R_Z from a high limit to unity. However, even at 150,000 K the temperature ratio from this effect is still under 1.2. The observed picture is at least consistent with blackbody energy distributions and variations in optical depth.

From the plots in Kaler (1983*b*) we see that R_Z can be unity for nebulae with $I(\lambda3727) = 100F(\lambda3727)/F(\mathrm{H}\beta) \gtrsim 100$, and that for most objects with $I(3727) > 100$, R_Z is under 1.5. We establish this line intensity as our initial criterion for high optical depth and test the results later. Obviously, the criterion will cause us to include a few objects with large R_Z, resulting in false, and too high, values of temperature. We can establish similar criteria for λ6583, but because nitrogen can be strongly enriched in planetaries, we must be more conservative. For an N/O ratio of 0.26, a typical low value, $I(\lambda3727) = 100$ corresponds to $\mathrm{N}/\alpha = F(\lambda6584)/F(\mathrm{H}\alpha) = 0.20$ (derived from stan-

dard abundance procedures and $T_e = 10{,}000$ K). Allowing for a factor of 5 enrichment in nitrogen we select $N/\alpha = 1$ as a secondary criterion, which is consistent with the empirical plot of N/α versus R_Z in Kaler (1983*b*).

c) Data

In order to develop a working list of objects, we combed the literature to find those with $I(\lambda 3727) \geq 100$ and $N/\alpha \geq 1$. Our preference was always for global values, that is, ratios derived from total fluxes. Otherwise we averaged all available small-aperture data so that we could obtain some sense of a global value. (That is, we did not simply look for one observation that could put the ratio over the limit.) Data were taken from Kaler's (1976*b*) catalog of emission-line intensities, references to individual objects listed by Kaler (1983*c*), plus compilations by Kondratyeva (1978), Aller and Czyzak (1979, 1983), Aller and Keyes (1987), Gutiérrez-Moreno, Moreno, and Cortés (1985), and Kaler, Shaw, and Kwitter (1989), with global values from Kaler (1983*a*, *b*) and Shaw and Kaler (1989). The Gutiérrez-Moreno, Moreno, and Cortés values are considered to be global as well. Unpublished Steward Observatory data were also used for one object (M1-8).

The resulting list of objects, their associated data, and results are all presented in Table 1, beginning with NGC, continuing with IC, and then alphabetically. The second, third, and fourth columns give the information necessary for the calculation of the temperatures. They are generally taken from an upcoming compilation by Cahn and Kaler (1989). The Hβ fluxes, $F(\mathrm{H}\beta)$, are compiled (and corrected to the modern photometric standard) from references listed by Shaw and Kaler (1989), as well as from that paper itself (see their § III*a*). The He II $\lambda 4686$ intensities in column (3) come from the references cited above for the optical depth criteria and include the global values of Kohoutek and Martin (1981*a*). Nonglobal values are indicated by footnote "*b*." The interstellar extinction constants c (logarithmic extinction at Hβ) are, except in a few cases, derived from Hα/Hβ intensity ratios and the Whitford (1958) extinction function (for which f_λ, in standard nebular notation, is -0.335). The references are the same as above, with the addition of Dufour (1984), Kaler (1985*b*), Kaler, Pratap, and Kwitter (1987), and Kaler, Chu, and Jacoby (1988).

The next two columns give the relative $\lambda 3727$ and $\lambda 6583$ intensities used as depth criteria. Nonglobal values, which are always somewhat suspect, are indicated by a footnote. *The* [O II] $\lambda 3727$ *intensities are corrected for reddening* ($f_\lambda = 0.30$); the $\lambda 6583$ line is so close to Hα that no correction is necessary. With three exceptions (NGC 6302, NGC 7027, and A71) all nebulae for which there are [O II] observations have $I(\lambda 3727) > 100$. NGC 7027 is generally considered as thick; the [O II] and [N II] lines are suppressed by high density. The other two objects are included because N/α is high, as is N/O, and we thought an upper limit on temperature would be of interest. For eight nebulae, no value of $I(\lambda 3727)$ is available, and the depth decision rests upon N/α alone. For those objects in this class observed by Shaw and Kaler (1989) (NGC 2899, NGC 3195, NGC 5189, Hal-3, and He2-120), the N/α ratio could be too high due to the convolution of their Hα and [N II] filters. Therefore nebulae with N/α close to one *may* be suspect. The resulting uncertainty in Hα for these five nebulae (plus He2-114) renders their values of c uncertain. NGC 3699 is also included to provide an upper limit on temperature. In a small number of cases (He2-15 and M1-40) some of the basic data were taken from unpublished Kitt Peak and Steward Observatory data. Note that these line ratios are not generally suitable for calculations of N/O abundance ratios, as there may be no correlation between the nebular regions observed (one may be global, the other not).

As the last of the input data, column (7) gives the angular radii of the nebulae, ϕ, in seconds of arc. These will be used below for estimates of distance (actually upper limits to distance), and are taken from Perek and Kohoutek (1967). In the cases of double shell nebulae, we generally adopt only the smaller of the two (for NGC 2440 we use a larger, and for NGC 6781 we use a mean).

d) Procedure

We next calculate the expected visual magnitude, temperature, and luminosity from the Zanstra program described by Kaler (1983*b*), which uses the Harman-Seaton formulation. The star is considered to be a blackbody, and the Stasińska-Tylenda effect is not included. Ordinarily, one puts in V (and/or B) and the code calculates the Zanstra temperature, T, the Shklovsky distance, D (Cahn and Kaler 1971), and the resulting luminosity. We modified the program to adopt an initial low magnitude for the calculation of $T_Z(\mathrm{H})$ and $T_Z(\mathrm{He\ II})$, and then to step upward until they cross. The results are presented in columns (8), (9), (10), and (11). *Since the nebulae are (almost) all considered to be optically thick, the Shklovsky distances and the resulting luminosities must generally be regarded as upper limits.*

T(cross) and V(cross) can be presented in simple graphical and polynominal form. In Figure 1 we plot T(cross) against I_c ($\lambda 4686$), where the intensity is on the usual scale of $I(\mathrm{H}\beta) = 100$ and is corrected for reddening. A polynominal fit to the curve for $8 < I_c < 100$ yields

$$\log T(\mathrm{cross}) = 4.905 + 1.11162 \times 10^{-2} I_c(\lambda 4686) - 1.10692 \times 10^{-4} I_c{}^2(\lambda 4686) + 6.20572 \times 10^{-7} I_c{}^3(\lambda 4686)\ . \quad (1)$$

The equation is good to at worst 1500 K, well within methodological error. Below $I = 8$, the curve must be used. The difference between V(cross) and the nebular Hβ flux expressed as a

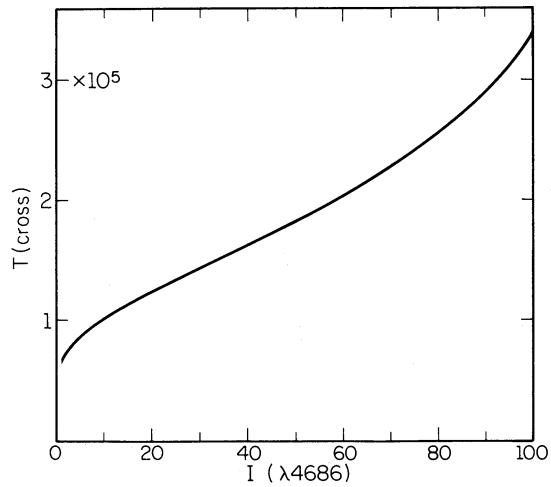

FIG. 1.—T(cross) for stars of optically thick nebulae plotted against the unreddened intensity of He II $\lambda 4686$, $I(\lambda 4686)$, which is on the scale of $I(\mathrm{H}\beta) = 100$.

TABLE 1

CROSSOVER MAGNITUDES AND TEMPERATURES

Nebula (1)	$-\log F_0(H\beta)$ (2)	I_0 (λ4686) (3)	c (4)	I_c[a] (λ3727) (5)	N/α[a] (6)	ϕ (7)	D(kpc)[b] (8)	V(cross) (9)	10^3 T(K) (10)	L/L_0[b] (11)	V(obs) (12)	N/O (13)	Reference for N/O (14)
NGC 650	10.68	54[c]	0.20	650	2.16[c]	36	1.1	17.89	192	210	17.5 (1)	0.50	1
NGC 2438	11.04	41	0.20	448	0.66[c]	35	1.3	18.44	165	120	17.22(2) 17.9 (3) 18.4 (4)	0.34	1
NGC 2440	10.50	65	0.32	158	3.86	30	1.1	17.70	219	440	17.6 (5) 17.72(6)	2.4	2, 3
NGC 2474	11.27	28	0.00	258	2.1	194	0.58	18.67	139	7	17.43(3)	1.2	1
NGC 2818	11.29	66	0.30	326[c]	1.68	20	2.0	19.71	221	240	19.58(2) 19.5 (4)	1.1	3, 4
NGC 2867	10.59	30	0.43	110	0.23	6	2.8	16.93	145	2300	16.66(2) 16.5 (4) 15.0 (7) 14.5 (8)	0.25	2, 5
NGC 2899	11.35	79	1.29[d]	...	2.79	60	0.67	20.09	285	285	...	...	...
NGC 3195	11.06	10	0.65[d]	420[c]	1.13	19	1.6	17.17	103	335	16.1:(7)	0.25	5
NGC 3587	10.42	11	0.01	327[c]	0.65[c]	100	0.58	15.81	104	46	16.04(9)	0.28	1
NGC 3699	11.21	77	0.64	...	0.88	35	1.2	19.76[e]	260[e]	250	...	...	...
NGC 5189	10.79	47[c]	0.85[d]	...	1.03[c]	70	0.58	17.84	183	195	14.75(2) 14.0 (10)	...	...
NGC 6302	10.55	62[c]	1.13[f]	67[c]	1.48[c]	23	0.89	17.60[e]	224[e]	1780	20.7 (2)	5.2:	6
NGC 6445	11.22	50[c]	0.25[f]	240[c]	...	17	2.2	19.13	184	255	18.72(2) 18.9 (10)	1.2	1
NGC 6537	11.40	65	2.11	119	1.18	55	0.51	19.67	250	745	19.0 (10)	0.9	7, 8, 9
NGC 6565	11.22	12	0.41	478[c]	...	5	4.2	17.76	108	980	19.2 (10) 15.88(7)	0.48	10, 11
NGC 6620	11.74	29	0.80	152[c]	0.82	2.3	7.1	19.68	145	2480	...	0.43	12
NGC 6720	10.08	39[c]	0.29	605[c]	1.30[c]	36	0.80	15.96	162	485	15.00(9)	0.35	13
NGC 6741	11.35	45[c]	0.96	180[c]	0.95[c]	4	4.0	19.16	180	3180	20.0 (2)	0.59	14, 15
NGC 6772	11.67	31[c]	0.93	290[c]	1.06[c]	32	1.3	19.54	150	140	18.63(2) 18.9 (10) 19.0 (11)	...	...
NGC 6781	11.21	13[c]	1.02	586[c]	1.47[c]	55	0.7	17.63	112	130	16.62(2) 14.95(9)	0.38	12, 16
NGC 6853	9.46	33[c]	0.18	608[c]	1.78[c]	208	0.22	14.26	150	110	14.0 (1) 13.82(9)	0.36	17
NGC 6881	12.26	25	2.04	135	0.70	1.5	6.6	20.53	143	11100	16.7 (12) 16.4 (13)	0.50	7, 18
NGC 6886	11.31	40[c]	0.76	160[c]	0.60[c]	3	5.1	18.96	168	3410	...	0.34	19
NGC 6894	11.41	8	0.88	122	0.78	21	1.6	17.83	98	250	17.9 (11)	0.99	12
NGC 7027	10.12	41	1.24	27[c]	0.36[c]	7	1.4	15.91	174	12700	16.2 (5) 16.32(14)	...	...
NGC 7048	11.41	46[c]	1.00	...	1.26[c]	31	1.2	19.33	183	275	18 (15)	...	...
NGC 7139	11.80	14[c]	0.76	379[c]	1.46[c]	39	1.4	19.23	113	62	19.8[g](16) 18.1 (11)	0.63	16
NGC 7293	9.37	10	0.04	395	...	403	0.15	13.11	102	38	13.43(9)	0.17	16
IC 972	12.04	20	0.00	260	0.54	24	2.9	20.31	124	29	18.16(2) 18.2 (11) 18.4 (17)	0.28	1
IC 4406	10.76	7[c]	0.28	618[c]	1.42	10	2.4	16.29	94	640	17.58(2)	0.36	3
A2	12.37	61	0.59	125[c]	0.27	15.5	3.3	22.22	213	105	20.2 (11) 19.8 (17)	0.32	1, 16
A31	10.54	32	0.00	225	0.60	486	0.24	16.98	147	7	15.51(17)	0.40	1
A50	12.02	34	0.00	105[c]	0.28[c]	13.5	4.0	20.74	151	68	19.8 (17)	0.40	1
A70	12.34	46	0.07	113[c]	0.80	21	3.5	21.86	174	32	19.1 (11) 18.9 (17)	0.54	16
A71	11.75	29	1.12	91	1.50	79	0.74	19.63[e]	147[e]	55	18.95(17)	2.4	1
A82	11.72	15	0.79	360	0.93	47	1.2	19.07	116	58	...	0.36	1, 16
A84	11.74	17	0.33	385	0.83	66	1.2	19.34	119	20	18.49(17)	0.51	16
BV 1	12.62	65	1.37	175	1.19	22	2.1	22.8	236	155	...	1.45	20
Hal-3	12.93	66	2.99[d]	...	1.08	8	2.1	23.41	278	3710	...	...	...
Hel-6	12.19[h]	17	0.95	...	1.25	11	3.2	20.30	121	220	...	...	...
He2-15	12.33	53	1.98	298[c]	2.75:	10	2.2	21.63	211	1270	...	1.79	21
He2-114	12.28	22	1.64[d]	813[c]	1.13	15	2.0	20.56	135	375	...	0.26	5
He2-120	12.22	13	2.10[d]	...	1.05	15	1.6	19.86	115	705	...	...	...
Hul-1	11.60	9	0.41	425[c]	0.90[c]	2.5	7.6	18.51	100	1290	...	0.26	13, 19
Kl-1	12.36	33	0.28	...	4.26[c]	22	3.1	21.49	150	36	...	...	...
K1-7	12.13	13	0.15	256[c]	0.93	17	3.4	20.16	109	45	20.5 (11) 19.8 (17)	0.43	16
K2-2	11.12	7	0.00	108	0.25	207	0.52	17.26	93	7	15.0?(18)	0.34	1

TABLE 1—*Continued*

Nebula (1)	$-\log F_0(H\beta)$ (2)	I_0 (λ4686) (3)	c (4)	I_c[a] (λ3727) (5)	N/α[a] (6)	ϕ (7)	D(kpc)[b] (8)	V(cross) (9)	10^3 T(K) (10)	L/L_0[b] (11)	V(obs) (12)	N/O (13)	Reference for N/O (14)
K3-73	12.64[h]	20[c]	0.0:	288[c]	0.32[c]	8	7.3	21.18	124	50	21.2[g](16)	0.16	16
K3-74	13.36[h]	36	0.83	255[c]	0.68[c]	10	6.1	23.95	160	50	...	...	...
K3-86	13.62[h]	71[c]	1.14	310[c]	0.29[c]	4.7	9.4	25.54	251	195	21.1[g](16)	0.14	16
K3-91	14.54[h]	37[c]	2.06	693[c]	1.82[c]	2.9	12.5	26.65	171	250	19.6[g](16)	0.48	16
K3-92	13.50[h]	14[c]	1.37	417[c]	0.68[c]	3.65	9.3	23.31	115	240	20.6[g](16)	0.33	16
M1-7	12.05	15	0.78	226	1.17	4	5.5	19.90	116	610	...	0.48	7, 22
M1-8	12.37	37[c]	0.64	272[c]	1.39[c]	10	4.2	21.55	161	155	...	1.2	22, 23
M1-79	11.73	11	0.82	266	1.07	16	2.2	18.86	106	210	...	0.45	7
M2-51	11.97	13[c]	1.03	795	2.35	21	1.9	19.52	112	150	19.7[g](16)	0.41	16
M2-53	12.87[h]	26[c]	1.33	727[c]	1.42[c]	7.5	4.6	22.27	142	260	21.2[g](16)	0.27	16
M2-55	12.16	4	1.24	610	1.28	25	1.7	19.18	85	110	21.0[g](16)	0.31	16
M3-2	12.61	80	0.50	210[c]	3.91	4	8.7	23.36	267	410	16.96(7)	2.0	16
M3-3	12.29	11	0.56	337[c]	4.97	6.4	5.5	20.33	105	205	...	1.2	16
Mz 1	11.31	27	0.35	252[c]	...	17	2.2	18.65	139	210	...	...	...
Ym 29	10.40	26	0.27	217	1.27	319	0.25	16.36	137	20	15.99(17)	0.96	1, 24

[a] $I(\lambda 3727)$ is corrected for interstellar extinction. Other data are as observed. $N/\alpha = I(\lambda 6583)/I(H\alpha)$.
[b] Upper limits by definition of this technique.
[c] Not global.
[d] High error, ±0.4, in Shaw and Kaler's extinction as a result of high N/α. Extinction for He2-15 (which has a Shaw and Kaler N/α) is from unpublished IIDS data.
[e] Nebula does not quite meet optical depth criteria. Included to provide limit on V and T. Objects with no λ3727 and low N/α may also be suspect.
[f] Extinction from Hγ/Hβ and/or Hδ/Hβ, and not as reliable as others.
[g] Approximate and unreliable magnitudes from KSK, average of V and color-corrected B: not plotted.
[h] Flux from KSK surface brightness data, error of ±0.2 or greater.

MAGNITUDE REFERENCES.—(1) Cudworth 1973; (2) Gathier and Pottasch 1988; (3) Kaler and Feibelman 1985; (4) Walton *et al.* 1986; (5) Heap and Hintzen 1990; (6) Jacoby 1988*a*; (7) Shaw and Kaler 1989; (8) Martin 1981; (9) Shao and Liller 1973; (10) Reay *et al.* 1984; (11) Kohoutek in Perek and Kohoutek 1967; plus 0.5 mag, corrected to V; (12) Shaw and Kaler 1985; (13) Kohoutek and Martin 1981*b*; (14) Jacoby 1988*b*; (15) Hubble 1921; (16) Kaler, Shaw, and Kwitter 1989; (17) Abell 1966 (photographic values converted to V); (18) Kwitter, Jacoby, and Lydon 1988.

REFERENCES FOR N/O.—(1) Kaler 1983*b*; (2) Gutiérrez-Moreno *et al.* 1985; (3) Torres-Peimbert and Peimbert 1978; (4) Dufour 1984; (5) unpublished 2D-Frutti data from Shaw and Kaler; (6) Aller and Czyzak 1978; (7) Kaler 1983*a*; (8) Kaler 1985*b*; (9) Feibelman *et al.* 1985; (10) Kaler, Aller, and Czyzak 1976; (11) Kohoutek and Martin 1981*b*; (12) Aller and Keyes 1987; (13) Barker 1980; (14) Aller, Krupp, and Czyzak 1969; (15) Kaler and Lutz 1985; (16) Kaler, Shaw, and Kwitter 1989 (KSK); (17) Barker 1984; (18) Kaler, Pratap, and Kwitter 1987; (19) Aller and Czyzak 1979; (20) Kaler, Chu, and Jacoby 1988; (21) unpublished IIDS data from Kwitter and Kaler; (22) unpublished Steward Observatory data; (23) Kondratyeva 1978; (24) Kwitter, Jacoby, and Lawrie 1983.

magnitude, or V(cross) + 2.5 log $F(H\beta)$, is also a simple function of $I(4686)$, and is shown *for zero reddening* in Figure 2. A polynomial fit (again for $8 < I < 100$) gives

$$\begin{aligned} V_o(\text{cross}) = &-10.889 + 6.850 \times 10^{-2} I_c(\lambda 4686) \\ &- 6.7072 \times 10^{-4} I_c{}^2(\lambda 4686) \\ &+ 3.4423 \times 10^{-6} I_c{}^3(\lambda 4686) \\ &- 2.5 \log F_o(H\beta) - 0.35c\ , \end{aligned} \quad (2)$$

where V_o and F_o are *observed* (reddened) values, I_c is the intensity *corrected* for reddening, and c is the extinction constant. V(cross) is also expressible in terms of temperature as

$$\begin{aligned} V_o(\text{cross}) = &-86.74 + 24.402 \log T(\text{cross}) \\ &- 1.8242\ [\log T(\text{cross})]^2 \\ &- 2.5 \log F_o(H\beta) - 0.35c\ . \end{aligned} \quad (3)$$

The equations give V(cross) to within about 0.15 mag for equation (2) and 0.05 mag for equation (3). Below $I(\lambda 4686) = 8$, or $T_c < 90{,}000$ K, the curve must again be used.

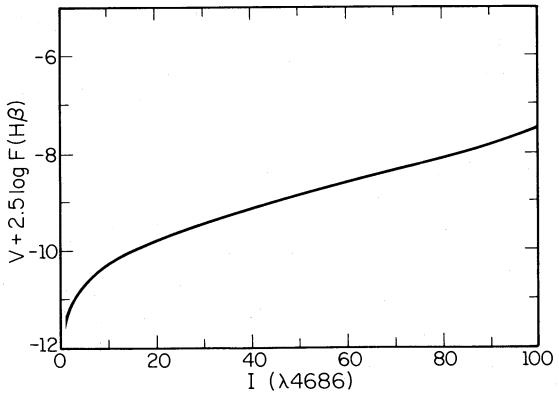

FIG. 2.—V(cross) + 2.5 log $F(H\beta)$, the visual magnitude of the central star plus the nebular Hβ flux expressed in magnitude form, for optically thick nebulae plotted against $I(\lambda 4686)$. All quantities are for zero reddening.

e) *Tests of the Results*

The obvious test is whether or not the predicted magnitudes in column (8) actually agree with the observed values. Stellar magnitudes have been observed for a surprising number of these planetaries—about 60%. They are listed in column (12) of Table 1, with references keyed at the bottom. In a few cases B (or photographic B) magnitudes were converted to V with $(B-V)_o = -0.4$, the extinctions in column (4), and $E(B-V) = c/K$, where K changes from 1.38 at $c = 0$ to 1.55 at $c = 1.0$ (see Kaler and Lutz 1985). We also converted a few of Gathier and Pottasch's (1988) λ4793–λ4866 magnitudes not already so done to V via their magnitude difference versus $E(B-V)$ relation, and converted Martin's (1981) λ5306 flux for NGC 2867 to V. We plot the results in Figure 3, with the points that represent the stars coded according to the way in which the observations were made: circles for photoelectric, boxes for imaged, crossed boxes for imaged with continuum

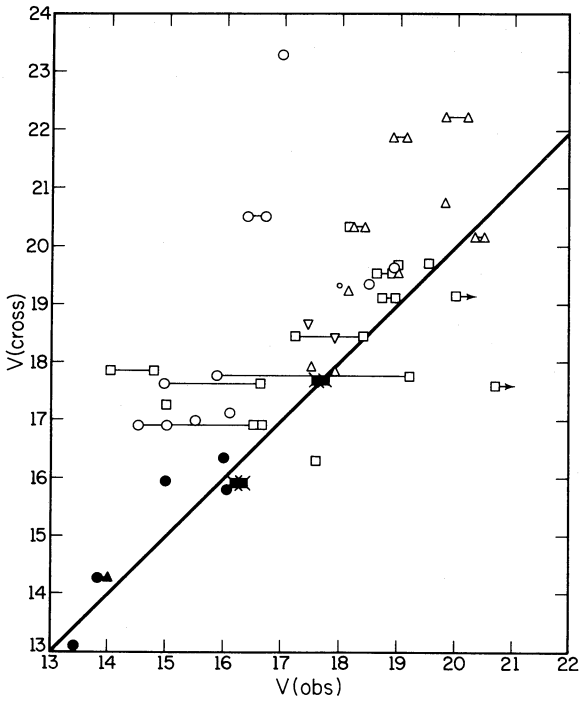

FIG. 3.—The predicted V(cross) plotted against the observed visual magnitudes, V(obs), from Table 1. *Circles*: photoelectric data; *boxes*: magnitudes derived from imaging; *crossed boxes*: imaging with continuum subtraction; *upward triangles*: photographic magnitudes; *downward triangles*: V derived from UV observations; *small dot*: crude estimate; *solid line*: 45° line for perfect agreement. Different magnitude measurements for one star are connected by a horizontal bar. The seven best objects given in the text are represented by filled symbols.

subtraction, upward triangles for photographic, downward triangles for V derived from UV observations, and a small filled dot for a crude estimate (NGC 7048). Multiple observations are connected by a bar. Two stars (NGC 6741 and NGC 6302) are plotted as limits.

The correlation between predicted and observed magnitudes is strong and very convincing. Our procedure works and our criteria appear to be reasonably appropriate. However, all is not perfect. Four stars fall way off the 45° (*solid*) line, M3-2, NGC 5189, NGC 6302, and NGC 6881. Shaw and Kaler's (1989) magnitude for the first may be in error: they indicate possible contamination from field stars: NGC 5189 is a marginal object with no observed λ3727, and may well be optically thin (see § IIc). At $V = 20.7$ for NGC 6302, the Zanstra code will not converge to a solution, and even at $V = 19.7$, R_Z is an unrealistic 0.73. We conclude that the observed magnitude limit determined for this object is incorrect, possibly as a result of the very high surface brightness or internal dust (Ashley and Hyland 1988). Note that these authors also estimate a temperature of 430,000 K from the silicon line strengths, far above the T(cross) of 224,000 K, which should be an upper limit, further showing the difficulties presented by this object. We exclude these three comparisons from further consideration.

The general distribution of points also tends to lie roughly one-half to three-quarters of a magnitude above the 45° (*solid*) line. There is a real possibility that some of the difference is due to erroneous observed magnitudes. They are notoriously hard to measure because of the bright nebular background, and large differences in the literature among observed values are well documented (see Shaw and Kaler 1985, 1989). Let us focus on what are likely to be the best observed values: those for the large nebulae with $V < 16.5$, for which the nebular continuum is not significant (NGC 3587, 6720, 6853, 7293, Ym 29), and the two derived from imaging with nebular continuum subtraction (NGC 2440 and NGC 7027), which are shown in Figure 3 by crossed boxes. Remarkably, these latter two stars were until recently not even detectable, and now the results appear free of systematic error: see the papers listed in Table 1 and note the agreement between the two independently derived values for each of them. Now, restricting the sample to these seven objects, which are indicated by filled symbols, we see that they follow the 45° line very well: the mean ΔV is only +0.15 mag, not significantly different from zero. In addition, no systematic effect with magnitude is present. We therefore conclude that our predicted magnitudes are generally reasonable and realistic (at least to magnitude 18), possibly a few tenths too faint on the average, and in some cases are quite likely to be superior to the observed magnitudes. Only improvements in the observations can test this contention.

Now, however, let us return to the full data set, with its $\frac{1}{2}$–$\frac{3}{4}$ magnitude upward offset, and examine some other possibilities that may cause it. First, our selection criteria may not be stringent enough, and we may have let a number of optically thin nebulae slip through (quite possible: see Kaler 1983*b*). Second, the Zanstra discrepancy may be produced at least in part by a UV excess. It would seem that at minimum we could rule out the Stasińska-Tylenda effect, since it would produce predicted magnitudes that are to bright rather than too faint. However, it could still exist and just be cancelled or even offset by a larger UV excess.

In order to examine the first possibility, we plot $\Delta V = V$(cross) − V(obs) against log $I(\lambda 3727)$ in Figure 4. If our criteria for depth are too low, we might expect to see the mean ΔV begin high at $I(\lambda 3727) = 100$ and decrease to zero as the [O II] intensity increases. Such an effect may actually be seen. Although the number of points in Figure 4 is too small for really definitive distinctions to be made, those with $I(\lambda 3727) < 150$ appear to have a mean ΔV higher than those with higher [O II] strengths. This higher [O II] criterion may be more appropriate. However, the seven best objects listed above, and filled in Figure 4, lie very nicely along the $\Delta V = 0$ line, with no systematic effect visible. Even the higher criterion does not absolutely ensure uniform optical thickness. The nebula may be constructed so as to leak radiation in one direction—say along a minor axis—with the result that T(cross) and V(cross) would be overestimated.

Above $I(\lambda 3727) = 150$, ΔV for the whole set is still generally positive, with a median of about 0.4 mag. A UV excess is consequently still a real possibility, especially if coupled with the Stasińska-Tylenda effect. We evaluate the latter in Figure 5, where we plot ΔV against T(cross). If the effect were solely operating, we should expect to see ΔV become more negative as temperature increases. The scatter of points is very large, and no clear correlation is evident. There may be a steady decrease between 120,000 K and 250,000 K but it is toward ΔV = zero rather than below it. No systematic shift is evident if we look only at the seven best stars, whose symbols are again filled in the figure. The effect may not be a factor since Stasińska and Tylenda's models were for densities higher than are generally appropriate for our nebulae.

If we can rule out the Stasińska-Tylenda effect, the UV excess cannot be very large, even if ΔV is 0.5 magnitudes or so. If we lower V(cross) by 0.5 magnitudes, R_Z increases on the

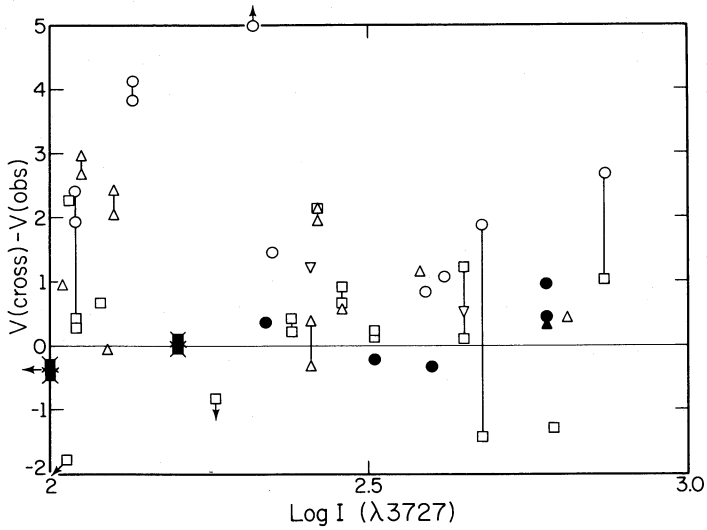

FIG. 4.—$\Delta V = V(\text{cross}) - V(\text{observed})$ plotted against log I([O II] λ3727), with the same symbolism as used in Fig. 3. Three extreme stars fall off the figure, M3-2 ($\Delta V = 6.4$) to the top, NGC 6302 [$\Delta V < -3.1$, log $I(\lambda 3727) = 1.83$] down and to the left, and NGC 7027 [log $I(\lambda 3727) = 1.43$].

average to 1.1, the exact amount depending slightly on temperature. As examples, T_Z(He II) for NGC 2440 (at the high end) drops from T(cross) = 219,000 K to 193,000 K and T_Z(H) to 176,000 K; NGC 3195 falls from T(cross) = 103,000 K to T_Z(He II) = 96,000 K and T_Z(H) to 86,000 K. Even at $\Delta V = 0.75$ magnitudes, R_Z climbs only to 1.2: for NGC 2440 T_Z(He II) and T_Z(H) respectively are then 182,000 K and 159,000 K; for NGC 3195 the corresponding numbers are 93,000 K and 79,000 K. These values for NGC 2440 are similar to the 166,000 K that Shields *et al.* (1981) need in order to model the nebula's ionization structure. But the star would have to be a full magnitude brighter than observed to reduce T_Z(He II) to that value. Given that the Stasińska-Tylenda effect is not a factor, the comparison between V(cross) and V(obs) constrains any UV excess to small amounts, with $R_Z < 1.2$, similar to the limit we adopted in § II*b*. The value is certainly smaller than the factor of 2 seen for the Méndez *et al.* (1988) sample (Kaler 1989). However note the possibility of a selection effect: there is only one object in common—NGC 7293—

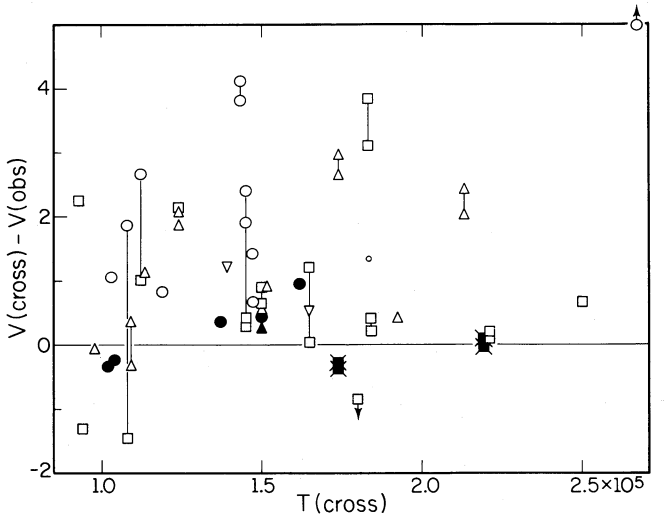

FIG. 5.—$\Delta V = V(\text{cross}) - V(\text{observed})$ plotted against T(cross) with the same symbolism as in Fig. 3. One star, M3-2 ($\Delta V = 6.4$, $T_* = 267{,}000$ K), falls off the diagram.

between the two sets. The optically thick nebulae, with strong [O II] and [N II], may simply have stars that are systematically different from those of other sets of objects.

We cannot entirely rule out combinations of effects that may produce false agreement between predicted and observed magnitudes. Nevertheless, the above tests provide credibility to the method and to the temperatures and magnitudes derived for the remaining 28 planetaries for which the star is not observed (including those from Kaler, Shaw, and Kwitter 1989, labeled with footnote "g"), and for the one for which V is only a rough estimate (NGC 7048). The acid test will now be to find and observe the nuclei of these 28 (and of course to improve the magnitudes for several of the others) to see really how well our predictions fare and to uncover any correlations that may be hidden in the present scatter.

III. ANALYSIS

a) Temperature Distribution

Not surprisingly, all the stars are hot, ranging from a low of 85,000 K for M2-55 up to 255,000 for NGC 2899. As hot as the high limit is, the value is not out of line. The highest with observed V magnitudes are NGC 6537, NGC 2818, and NGC 2440, with T(cross) of 250,000 K, 221,000 K, and 219,000 K respectively. If we substitute the observed V we still derive 208,000, 211,000, and 217,000 for the three.

The distribution is best seen on the log L – log T plane of Figure 6, on which the stars are plotted from Table 1. Those for which $I(\lambda 3727) < 100$ (or for which λ3727 is not observed and N/α is low), for which T(cross) is likely to be an upper limit (footnote "d" in the table) are indicated with long rightward arrows. Those with $100 < I(\lambda 3727) < 150$ (unless $\Delta V < 1$ and again excluding NGC 7027) *may* be upper limits and are indicated by shorter arrows. Other symbolism will be discussed in § III*b*. On the figure, the evolutionary tracks for 0.6, 0.8, and 1.2 $M_\odot$ are taken from Paczyński (1971), that for 0.55 $M_\odot$ from Schönberner and Weidemann (1981: see Schönberner 1981), and that for 1.4 $M_\odot$ is an extrapolation of these by Shaw (1988). The stars are plotted according to the temperatures and luminosities of Table 1. Be aware, however, that *the log L are by definition and contention of this paper all upper limits.* Since

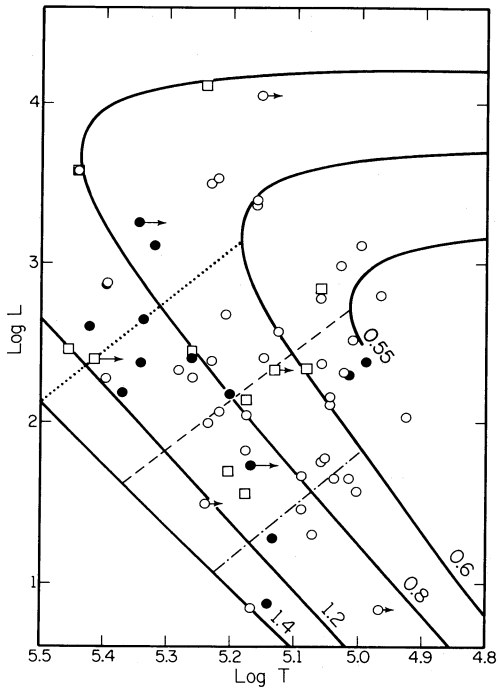

FIG. 6.—The predicted results plotted on the (log L – log T) plane, with Paczyński-Schönberner evolutionary tracks for various masses in units of $M_\odot$ (see the text). *The luminosities are upper limits.* The filled circles have enriched surrounding nebulae with N/O > 0.8, open circles N/O < 0.8. Boxes represent nebulae with unknown N/O. The lines cutting diagonally across the tracks are used to tie core mass to log T for theoretical comparisons (see the text and Fig. 4).

we have no idea of the ratio of ionized to total mass, we do not know how far downward from the plotted points their actual positions must be. But if the ratio is 0.5 [which since $I(\lambda 3727) = 100$ represents our transition point should not be far out of line], log L would be high by only 0.24 (since the Shklovsky distance scales as the nebular mass raised to the 0.4 power), displacing the points relatively little. Even if the ratio were 0.1, the points are high by only 0.8 in the log. The point of the discussion is that the luminous stars really are quite high in the figure and cannot mix with the dim ones, and that the low-luminosity stars truly are faint.

Nevertheless, real caution in using the luminosities is strongly advised (the distance scale constant may not be right either). It is not appropriate to use the positionings in Figure 3 to make too strong a statement about core mass distribution. However, the distribution in T(cross) alone does allow some limited conclusions because of the upper limits imposed on the luminosities. Selection effects are too great to allow any sort of real distribution, but we do see evidence for higher masses. Several stars congregate near the turnaround temperature of the 0.8 $M_\odot$ mass track, and the lower edge of the distribution (which could be lower yet) is roughly bounded by the 1.0–1.2 $M_\odot$ tracks. The latter figure could still be too high because of a scaling error in the distances.

b) A Test of Dredge-Up Theory

The most important use of these results is in a test of the ability of giant stars to dredge fresh nitrogen to their surfaces before they are expelled to form the planetaries. Various predictions that relate the enrichment in the nitrogen-to-oxygen ratio (N/O) to initial mass have been made by Becker and Iben (1979, 1980) and by Renzini and Voli (1981). Tests are usually done through comparison of the observed correlation between N/O and He/H with the predicted (Kaler 1983*c*, 1985*a*; Peimbert and Torres-Peimbert 1983; Aller 1983). The fits are more-or-less reasonable, the outstanding anomaly being the very high extreme He/H and N/O ratios that are not accommodated by theory.

More specifically, Kaler, Shaw, and Kwitter (1989, hereafter KSK) have related N/O directly to core mass (M_c) for a large sample of large planetaries with low-luminosity central stars. They find that N/O changes little if at all with core mass for $M_c \lesssim 0.8$, but above that figure it rises faster with M_c than predicted by the theory of Becker and Iben (1980). The chief criticism of their procedure is that the evaluations of core masses depend on distances.

We have an opportunity to test this theory with the sample of stars collected here, quite independently of the test produced by KSK, and more importantly, independently of distance. There is some overlap in the objects studied, but generally our stars are hotter than theirs, which cut off at log $T \approx 5.2$. Even given that the distance method we use is correct, we still cannot derive core masses from Figure 6, since our luminosities are upper limits. So instead, we use only temperature, *which in a statistical sense must be directly related to M_c for stars that are on descending tracks:* for a uniform distribution of stars, the average temperature of those with lower core masses must also be lower, as is evident from Figure 6. That way we can compare two quite independently determined quantities with one another, T(cross) and N/O. It is true that any one of our temperatures (and V predictions) may be wrong. What is important is that the derived values are statistically correct with little systematic error, as evidenced by Figures 3, 4, and 5. Then we can use the results for a statistically valid test.

The N/O ratios are listed in column (13) of Table 1, with the references to their sources in column (14), keyed at the bottom. In a few cases, the N/O were calculated from unpublished data using standard methods (see KSK or Kaler 1985*b*). We plot the results in Figure 7 as N/O versus log T(cross). The correlation is strong and very obvious: high-temperature nuclei, which tend to have the higher core masses, also have the higher nebular N/O, the correlation present at the 99.9% confidence level. It actually appears more as a step function with N/O climbing rather suddenly as log T passes a threshold. There are a few points that do not seem to fit well. If we identify and exclude the low-luminosity stars, log $L < 2$ (*filled symbols*), which narrows the relation between M_c and T(cross), the correlation between N/O and T(cross) improves. In fact, we appear to be able to see it in both the high- and low-luminosity sets of points. The low-luminosity set marginally appears to begin to climb at lower temperature, since high T means an even higher M_c at low L than at high L. The outstanding anomalies are now NGC 6894 at log $T = 4.99$, N/O = 0.97 and M3-3 at log $T = 5.02$, N/O = 1.2.

The N/O and T(cross) may be independently determined, but it is possible that there may be a linkage. The enriched type I nebulae (Peimbert and Torres-Peimbert 1978) tend to have a nonuniform structure (e.g., Kaler 1983*b*) and may leak some radiation along a particular direction thus causing us to overestimate the temperatures of their nuclei. More observed magnitudes are needed to evaluate this effect.

The correlation can be seen as well in Figure 6. There, we have filled in the symbols that represent stars that have highly enriched Type I nebulae, those with N/O > 0.8. Open circles

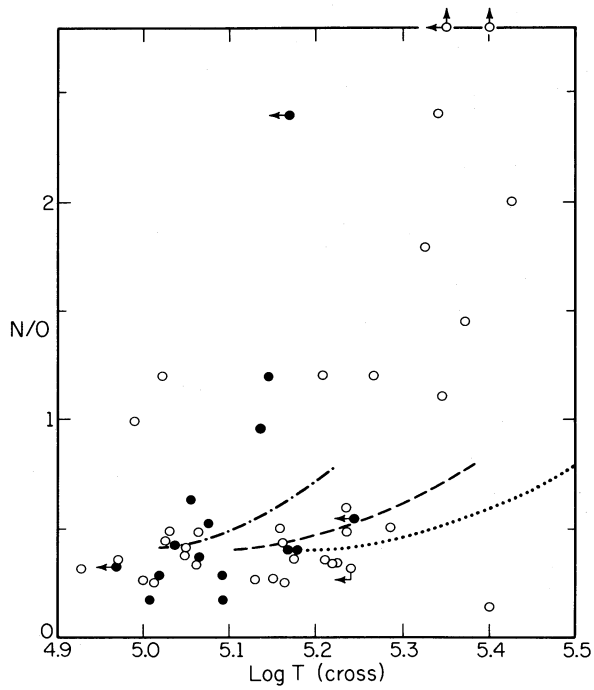

FIG. 7.—Nebular N/O from Table 1 plotted against log T(cross). The filled symbols have log L (upper limit) < 2. The three curved lines are theoretical loci based on the three analogous lines in Fig. 3 as described in the text. The dashed curve represents the mean, the dash-dot curve goes roughly with the filled symbols, and the dotted curve with the open.

represent those nebulae with low N/O, below 0.8. Boxes show nebulae with no measurements. We see that enriched nebulae concentrate toward higher M_c.

We can make a comparison with theory by relating temperature with core mass along the dashed line in Figure 6, which roughly represents the mean distribution of points. We use only one dredge-up scenario, that from Becker and Iben (1980) in which some C is converted to N after third dredge-up (their maximum N/O), which relates N/O to initial mass, M_i. We then relate M_i to M_c through the work of Iben and Truran (1978). The result is the dashed line in Figure 7, which we see is too low at high temperature and high core mass. If we divide the points in Figure 6 into high- and low-luminosity groups respectively along the dotted and dash-dot lines, we derive the similarly plotted curves in Figure 7.

The result is strikingly similar to that found by KSK. N/O changes little with increasing T(cross) at first, then accelerates as high values of T(cross) are approached. The dividing line (see Fig. 6) is consistent with that found by KSK, about 0.8 $M_\odot$. We also see that the qualitative relation between the high- and low-luminosity sets agrees with theory, that is the N/O versus log T(cross) correlation shifts to the left as luminosity falls. But again, standard dredge-up theory does not provide enough nitrogen, and the theory does not produce a fast enough climb in N/O with increasing core mass.

IV. CONCLUSIONS

The conclusions of this paper can be stated quite succinctly. First, our work shows that an ultraviolet excess does not seem to be a very big factor for these stars, and that the Stasińska-Tylenda effect, which involves interlocking between helium and hydrogen ionization, does not appear to be a significant factor even for very hot stars. The standard Zanstra method appears to give reliable temperatures, and Zanstra discrepancy can be explained largely by optical depth effects. The agreement between our predicted and the observed visual magnitudes provides a strong constraint on any UV excess shortward of 228 Å. Further progress in evaluating various effects relating to temperature must await improvements in the measurements of the magnitudes of these hot stars.

Second, we show indirectly the correlation that exists between core mass and chemical enrichment, which powerfully justifies the concepts of the current theory. Our analysis does show, however, that dredge-up theory does not go far enough. Additional enrichment from other burning situations, e.g., Renzini and Voli's (1981) hot bottom burning, must be invoked. In addition, the relation between initial and core masses may well be incorrect. The N/O versus log T curve could be made to climb faster if mass loss proceeded at a rate greater than that presented by Iben and Truran (1978), so that high initial mass resulted in lower core mass and lower log T.

The next obvious step, of course, is to see how good our predictions are by observing the stars with blanks (or indicators of uncertainty) in column (11) of Table 1. The next few years should tell how close we have come.

This research was supported by NSF grants AST 84-19355 and AST 88-13686 to the University of Illinois. We would like to thank the University of Illinois Research Board for an allotment of computer time, and S. R. Heap and P. M. Hintzen for communicating results in advance of publication, and the referee for useful suggestions.

REFERENCES

Abell, G. O. 1966, *Ap. J.*, **144**, 259.
Aller, L. H. 1983, *IAU Symposium 103, Planetary Nebulae*, ed. D. R. Flower (Dordrecht: Reidel), p. 1.
———. 1984, *Physics of Thermal Gaseous Nebulae* (Dordrecht: Reidel).
Aller, L. H., and Czyzak, S. J. 1978, *Proc. Nat. Acad. Sci.*, **75**, 1.
———. 1979, *Ap. Space Sci.*, **62**, 397.
———. 1983, *Ap. J. Suppl.*, **51**, 211.
Aller, L. H., and Keyes, C. D. 1987, *Ap. J. Suppl.*, **65**, 405.
Aller, L. H., Krupp, E., and Czyzak, S. J. 1969, *Ap. J.*, **158**, 953.
Ambartsumyan, V. A. 1932, *Pulkovo Obs. Circ.*, Vol. **8**, No. 4.
Ashley, M. C. B., and Hyland, A. R. 1988, *Ap. J.*, **331**, 532.
Barker, T. 1980, *Ap. J.*, **240**, 99.
———. 1984, *Ap. J.*, **284**, 589.
Becker, S. A., and Iben, I., Jr. 1979, *Ap. J.*, **232**, 831.
———. 1980, *Ap. J.*, **237**, 111.
Cahn, J. H., and Kaler, J. B. 1971, *Ap. J. Suppl.*, **22**, 319.
———. 1989, in preparation.
Clegg, R. E. S., and Seaton, M. J. 1983, in *IAU Symposium 103, Planetary Nebulae*, ed. D. R. Flower (Dordrecht: Reidel), p. 536.
Cudworth, K. M. 1973, *Pub. A.S.P.*, **85**, 401.
Dufour, R. J. 1984, *Ap. J.*, **287**, 341.
Feibelman, W. A., Aller, L. H., Keyes, C. D., and Czyak, S. J. 1985, *Proc. Nat. Acad. Sci.*, **82**, 2202.
Ferland, G. J. 1978, *Ap. J.*, **219**, 589.
Gathier, R., and Pottasch, S. R. 1988, *Astr. Ap.*, **197**, 266.
Golovatyi, V-V. 1987, *Astr. Zh.*, **64**, 724.
Gutiérrez-Moreno, A., Moreno, H., and Cortés, G. 1985, *Pub. A.S.P.*, **97**, 397.
Harman, R. J., and Seaton, M. J. 1966, *M.N.R.A.S.*, **132**, 15.
Harrington, J. P., Seaton, M. J., Adams, S., and Lutz, J. H. 1982, *M.N.R.A.S.*, **199**, 517.
Heap, S. R., and Hintzen, P. M. 1989, *Ap. J.*, in press.
Henry, R. B. C., and Shipman, H. L. 1986, *Ap. J.*, **311**, 774.
Hubble, E. P. 1921, *Pub. A.S.P.*, **33**, 174.
Iben, I., Jr., and Truran, J. W. 1978, *Ap. J.*, **220**, 980.
Iijima, T. 1981, in *Photometric and Spectroscopic Binary Systems*, ed. E. B. Carling and Z. Kopal (Dordrecht: Reidel), p. 517.
Jacoby, G. H. 1988*a*, private communication.
———. 1988*b*, *Ap. J.*, **333**, 193.

Kaler, J. B. 1976*a*, *Ap. J.*, **210**, 843.
———. 1976*b*, *Ap. J. Suppl.*, **31**, 517.
———. 1983*a*, *Ap. J.*, **264**, 594.
———. 1983*b*, *Ap. J.*, **271**, 188.
———. 1983*c*, in *IAU Symposium 103, Planetary Nebulae*, ed. D. R. Flower (Dordrecht: Reidel), p. 245.
———. 1985*a*, *Ann. Rev. Astr. Ap.*, **23**, 89.
———. 1985*b*, *Ap. J.*, **290**, 531.
———. 1989, in *IAU Symposium 131, Planetary Nebulae*, ed. S. Torres-Peimbert (Dordrecht: Reidel), p. 229.
Kaler, J. B., Aller, L. H., and Czyzak, S. J. 1976, *Ap. J.*, **203**, 636.
Kaler, J. B., Chu, Y.-H., and Jacoby, G. H. 1988, *A.J.*, **96**, 1407.
Kaler, J. B., and Feibelman, W. A. 1985, *Ap. J.*, **297**, 724.
Kaler, J. B., and Lutz, J. H. 1985, *Pub. A.S.P.*, **97**, 700.
Kaler, J. B., Pratap, P., and Kwitter, K. B. 1987, *Pub. A.S.P.*, **99**, 952.
Kaler, J. B., Shaw, R. A., and Kwitter, K. B. 1989, in preparation (KSK).
Kohoutek, L., and Martin, W. 1981*a*, *Astr. Ap. Suppl.*, **44**, 325.
———. 1981*b*, *Astr. Ap.*, **94**, 365.
Kondratyeva, L. N. 1978, *Astr. Zh.*, **55**, 334.
Kwitter, K. B., Jacoby, G. H., and Lawrie, D. G. 1983, *Pub. A.S.P.*, **95**, 732.
Kwitter, K. B., Jacoby, G. H., and Lydon, T. J. 1988, *A.J.*, **96**, 997.
Martin, W. 1981, *Astr. Ap.*, **98**, 328.
Méndez, R. H., Kudritzki, R. P., Herrera, A., Husfeld, D., and Groth, H. G. 1988, *Astr. Ap.*, **190**, 113.
Natta, A., Pottasch, S. R. and Preite-Martinez, A. 1980, *Astr. Ap.*, **84**, 284.
Osterbrock, D. F. 1974, *Astrophysics of Gaseous Nebulae* (San Francisco: Freeman).
Pacyński, B. 1971, *Acta Astr.*, **21**, 417.
Peimbert, M., and Torres-Peimbert, S. 1978, *IAU Symposium 76, Planetary Nebulae*, ed. Y. Terzian (Dordrecht: Reidel), p. 215.
———. 1983, in *IAU Symposium 103, Planetary Nebulae*, ed. D. R. Flower (Dordrecht: Reidel), p. 233.
Perek, L., and Kohoutek, L. 1967, *Catalogue of Galactic Planetary Nebulae* (Prague: Czechoslovakia Acad. Sci).
Preite-Martinez, A., and Pottasch, S. R. 1983, *Astr. Ap.*, **126**, 31.
Reay, N. K., Pottasch, S. R., Atherton, P. D., and Taylor, K. 1984, *Astr. Ap.*, **137**, 113.
Renzini, A., and Voli, M. 1981, *Astr. Ap.*, **94**, 175.
Schönberner, D. 1981, *Astr. Ap.*, **103**, 119.
Schönberner, D., and Weidemann, V. 1981, private communication.
Shao, C. Y., and Liller, W. 1973, private communication.
Shaw, R. A. 1988, in *IAU Symposium 131, Planetary Nebulae*, ed. S. Torres-Peimbert (Dordrecht: Reidel), p. 473.
Shaw, R. A., and Kaler, J. B. 1982, *Ap. J.*, **261**, 510.
———. 1985, *Ap. J.*, **295**, 537.
———. 1989, *Ap. J. Suppl.*, **69**, 495.
Shields, G. A., Aller, L. H., Keyes, C. D., and Czyzak, S. J. 1981, *Ap. J.*, **248**, 569.
Stasińska, G., and Tylenda, R. 1986, *Astr. Ap.*, **155**, 137.
Stoy, R. H. 1933, *M.N.R.A.S.*, **93**, 588.
Torres-Peimbert, S., and Peimbert, M. 1978, *Rev. Mexicana Astr. Ap.*, **2**, 181.
Walton, N. A., Reay, N. K., Pottasch, S. R., and Atherton, P. D. 1986, *New Insights in Astrophysics, Joint NASA/ESA/SERC Conf.* (ESA SP-263), p. 497.
Whitford, A. E. 1958, *A.J.*, **63**, 201.
Zanstra, H. 1927, *Ap. J.*, **65**, 50.

GEORGE H. JACOBY: Kitt Peak National Observatory, National Optical Astronomy Observatories, P.O. Box 26732, Tucson, AZ 85726

JAMES B. KALER: Department of Astronomy, University of Illinois, 349 Astronomy Building, 1011 W. Springfield Avenue, Urbana, IL 61801